A EUROPEAN JOURNAL OF CHEMICAL BIOLOGY

CHEMBIOCHEM

SYNTHETIC BIOLOGY & BIO-NANOTECHNOLOGY

Accepted Article

Title: From bugs to bioplastics: Total (+)-dihydrocarvide biosynthesis by engineered Escherichia coli

Authors: Gabriel A Ascue Avalos, Helen S Toogood, Shirley Tait, Hanan Messiha, and Nigel Scrutton

To be cited as: *ChemBioChem* 10.1002/cbic.201800606

Link to VoR: http://dx.doi.org/10.1002/cbic.201800606

A Journal of ChemPubSoc Europe

WILEY-VCH www.chembiochem.org

From bugs to bioplastics: Total (+)-dihydrocarvide biosynthesis by engineered *Escherichia coli*

Gabriel A. Ascue Avalos, Helen S. Toogood, Shirley Tait, Hanan L. Messiha and Nigel S. Scrutton*

Abstract: The monoterpenoid lactone derivative (+)-dihydrocarvide ((+)-DHCD) can be polymerised to form shape memory polymers. Synthetic biology routes from simple, inexpensive carbon sources are an attractive, alternative route over chemical synthesis from (*R*)-carvone. We have demonstrated a 'proof of principle' *in vivo* approach for the complete biosynthesis of (+)-DHCD from glucose in *E. coli* (6.6 mg/L). The pathway is based on the *Mentha spicata* route to (*R*)-carvone, with the addition of an 'ene'-reductase and Baeyer-Villiger cyclohexanone monooxygenase. Co-expression with a limonene synthesis pathway enables complete biocatalytic production within one microbial chassis. Successful production of (+)-DHCD was achieved by screening multiple homologues of the pathway genes, combined with expression optimisation via selective promoter and/or ribosomal binding site screening. This study demonstrates the potential application of synthetic biology approaches in the development of truly sustainable and renewable bioplastic monomers.

Introduction

The increasing popularity of non-petroleum based bio-polymer applications is driven by concerns over dwindling fossil fuel supplies and the environmental impact of non-biodegradable plastic waste accumulation.[1] Industrially-relevant biodegradable polymers include elastomers, resins and composites, which are often composed of cyclic ester monomers (lactones).[2] For example poly-ε-caprolactone[3] and polylactide[4] are employed in drug delivery and tissue engineering applications,[5] and are often major components in polyurethane biopolymers.[6] A variety of limonene-based monoterpenoids found in *Mentha* essential oils[7] can be converted into the lactone monomers menthide, carvomenthide and (+)-dihydrocarvide ((+)-DHCD).[8] Subsequent polymeric forms have uses as thermoplastic elastomers (shape memory polymers)[9] and pressure sensitive adhesive components.[8, 10]

Synthetic routes to monomeric (+)-DHCD production include hydrogenation and subsequent Baeyer-Villiger oxidation of the natural product (*R*)-carvone.[5a, 11] However, a synthetic biology route could serve as an alternative approach (Scheme 1), given that the enzymes responsible for (*R*)-carvone biosynthesis in *Mentha spicata* are known,[7] and prior studies with Baeyer-Villiger cyclohexanone monooxygenases (CHMO) have demonstrated (+)-DHCD production.[8, 12] An early attempt at *in vivo* (*R*)-carvone production was performed by incorporating the C5 isoprenoid precursor (geranyl pyrophosphate) production and subsequent spearmint pathway genes into recombinant *Escherichia coli*.[13] However this approach was unsuccessful due to severe limitations in limonene precursor availability. This was overcome by feeding the cultures with (*S*)-limonene, but was limited by precursor uptake and cytotoxicity issues.[13] A more recent study utilised orange peel as the limonene feedstock in mixed culture of two recombinant microorganisms containing the pathway genes for (1*S*,5*R*)-carveol and (+)-DHCD lactone biosynthesis, respectively.[12d] This was successful in generating (+)-DHCD from waste orange peel, however limonene cytotoxicity impacted on the upper levels of feedstock concentrations that could be applied.[12d] To overcome this cytotoxicity, another study designed a cell-free system for (*R*)-carvone production from glucose.[14] However, due to time constraints only limonene was efficiently produced.

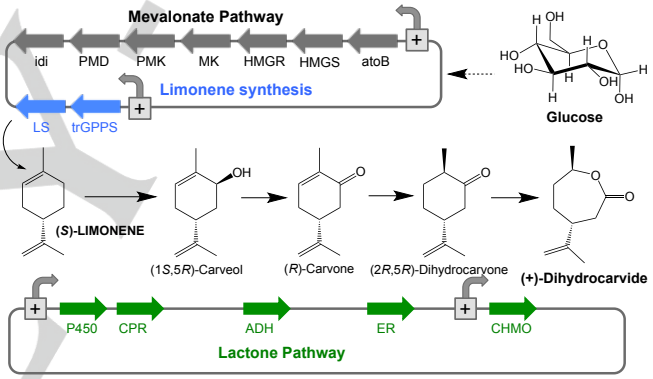

Scheme 1. Synthetic biology approach towards *in vivo* (+)-dihydrocarvide monomer biosynthesis in *E. coli*. Enzymes: atoB = acetoacetyl-CoA synthase; HMGS = hydroxymethylglutaryl-CoA synthase; HMGR = hydroxymethylglutaryl -CoA reductase; MK = mevalonate kinase; PMK = phosphomevalonate kinase; PMD = phosphomevalonate decarboxylase; idi = isopentyl diphosphate isomerase; trGPPS = N-terminally truncated geranyl pyrophosphate synthetase; LS = limonene synthase; P450 = limonene-6-hydroxylase; CPR = cytochrome P450 reductase; ADH = alcohol dehydrogenase; ER = ene-reductase and CHMO = cyclohexanone monooxygenase.

We propose a more direct route, where a *M. spicata*-like pathway to (*R*)-carvone production is combined with a specific CHMO within one recombinant strain of *E. coli* (Scheme 1). Limitations in C5 isoprenoid precursor production would be minimised by incorporating a second construct containing a eukaryotic mevalonate pathway, to enable lactone production from simple carbon sources.[15] The latter pathway was shown previously to substantially increase the *in vivo* production of the

G.A. Ascue Avalos, Dr H.S. Toogood, Dr H.L. Messiha, Prof. N.S. Scrutton
School of Chemistry, Faculty of Science and Engineering
University of Manchester
131 Princess Street, Manchester M1 7DN, U.K.
E-mail: nigel.scrutton@manchester.ac.uk

Supporting information for this article is given via a link at the end of the document.

limonene derivative perillyl alcohol in *E. coli*.[15a] Homologues and modifications of key enzymes were screened using *in vivo* reactions to develop an optimised pathway to (+)-DHCD. Functional pathway constructs underwent further modifications of the controlling elements (e.g. promoters) to enable significant levels of the terminal lactone product to be generated.

Results and Discussion

Limonene hydroxylation

The entry step into the *M. spicata* biosynthesis of (*R*)-carvone is the hydroxylation of (*S*)-limonene to (1*S*,5*R*)-carveol (Scheme 1), catalysed by the cytochrome P450 enzyme limonene-6-hydroxylase (L6H) with its electron transfer partner cytochrome P450 reductase (CPR).[16] We generated an N-terminally truncated and modified form of L6H, based on earlier studies,[17] to eliminate the signal sequence and increase soluble expression in *E. coli* ($L6H_m$). Unfortunately only a partial sequence was available for mint CPR (205 aa; GenBank: AW255332), from studies with expressed sequence tags (EST) from mint glandular trichomes.[18] However the CPR from *Salvia miltiorrhiza* (Chinese Sage; SmCPR) has a high amino acid sequence homology (92%) to the EST CPR sequence from mint. Additionally, early studies with native L6H showed hydroxylation occurs in the presence of a CPR from *Arabidopsis thaliana* (AtCPR).[17] Therefore we generated C-terminally His_6-tagged versions of both SmCPR and AtCPR to determine the best electron transfer partner for $L6H_m$.

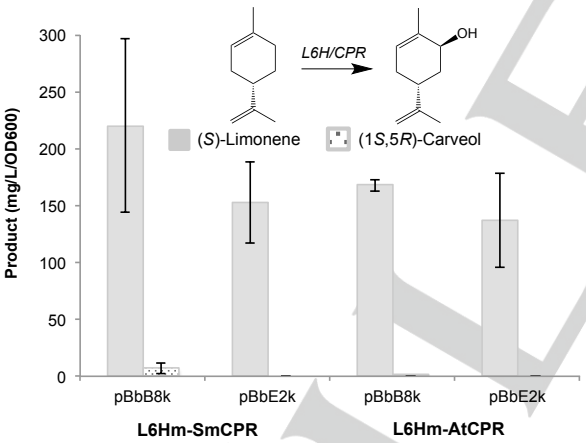

Figure 1. *In vivo* production of (*S*)-limonene and (1*S*,5*R*)-carveol by $L6H_m$-CPR constructs co-expressed with limonene synthesis plasmid pJE16410 in *E. coli*. Cultures (5 mL) were grown in Terrific broth, containing phosphate salts (9.4 g/L KH_2PO_4 and 2.2 g/L K_2HPO_4), 0.7 % (w/v) glucose, 60 μg/mL kanamycin and 100 μg/mL ampicillin. The culture was incubated at 37°C, 200 rpm until reaching OD600 = 0.4, followed by 25 μM IPTG (pJE16410), 500 μM δ-aminolevulinic acid, 25 μM arabinose (pBbB8k) or 100 nM tetracycline (pBbE2k) addition. The cultures were incubated at 30 °C for 72 hours. Each culture aliquot (1 mL) was cooled for 10 minutes on ice, followed by extraction of the nonane layer with ethyl acetate (2 x 375 μL) containing 0.01 % *sec*-butyl benzene. Product yields and identification were determined by GCMS analysis. OD_{600} of 1.0 corresponds to ~ 1.7 g/L wet weight of cells.[19] No detectable limonene hydroxylase activity was detected in control *E. coli* cells.

Initial co-expression constructs of $L6H_m$ with either SmCPR or AtCPR were generated in plasmid pCWori, under the control of a *tac* promoter.[17] *In vitro* biotransformations of cell lysates with limonene showed only poor (1*S*,5*R*)-carveol production by $L6H_m$ with either SmCPR or AtCPR over 24 h (e.g. 95.2 ± 3.3 μM with SmCPR; 1.9% yield; Supporting Information Figure S6). Therefore new $L6H_m$/CPR constructs were generated, with the C-His_6-tags removed, controlled by either *araBAD* (arabinose) or *tet* (tetracycline) promoters in different plasmid backbones (pBbB8k and pBbE2k, respectively). We performed *in vivo* reactions for the detection of functional $L6H_m$-CPR pairs instead of using purified proteins or cell lysates. This is due to difficulties in obtaining sufficient quantities of soluble, active membrane-associated $L6H_m$ (results not shown). This method involved the co-expression of $L6H_m$-CPR constructs with a limonene production plasmid pJBEI6410,[15a] thereby eliminating the need to supplement the culture with limonene. Cultures were grown in the presence or absence of a nonane overlay, which efficiently sequestered the monoterpenoids away from the aqueous phase to minimise cytotoxicity.

(*S*)-Limonene production was detected in all cultures, with a range of titres of 137-220 mg/L/OD_{600} dependent on the $L6H_m$-CPR construct (Figure 1). These differences likely reflect the efficiency of production vs the rate of utilisation by the expressed $L6H_m$/CPR, however the nature of the $L6H_m$-CPR plasmid backbone appeared to impact on limonene titres. The best (1*S*,5*R*)-carveol producing construct was $L6H_m$-SmCPR in pBbB8k (6.7 ± 4.3 mg/L/OD_{600}), with the equivalent AtCPR-containing plasmid showing a 20-fold reduction in yields (Figure 1). The higher than expected variability in (1*S*,5*R*)-carveol yields within replicates is a reflection on the non optimised growth and induction conditions, however a clear preference for the sage CPR was seen. No detectable levels of (1*S*,5*R*)-carveol were found with the constructs in the tetracycline-inducible pBbE2k plasmid. This could be indirectly related to the higher copy number and promoter strength, leading to changes in soluble recombinant protein expression levels and/or a higher metabolic burden on *E. coli*. This was seen by an increase in the relative proportion of insoluble protein expressed in these constructs (results not shown).

Optimisation trials were performed *in vivo* with the best performing construct $L6H_m$-SmCPR in pBbB8k co-expressed with the limonene production plasmid pJBEI6410. The parameters varied were the presence/absence of a *n*-nonane bilayer, culture density at induction, inducer concentration (IPTG and arabinose) and post induction time (Supporting Information Table S10). In contrast to studies with *in vivo* production of limonene and other monoterpenoids,[20] the presence of a *n*-nonane co-solvent reduced the levels of (1*S*,5*R*)-carveol production by at least 7-fold (1.7 ± 0.9 vs 12.8 ± 4.4 mg/L/OD_{600}). This is likely due to the sequestering of the (*S*)-limonene generated by the pJBEI6410 plasmid into the co-solvent, thereby reducing the intracellular concentrations and availability for the hydroxylation enzyme. Increasing the kanamycin concentration (selective for $L6H_m$-SmCPR) from 15 to 60 μg/mL led to a 3-fold increase in (1*S*,5*R*)-carveol. The best conditions leading to the highest yields of (1*S*,5*R*)-carveol were found to be

induction at an mid log phase, with 25 μM IPTG and 25 mM arabinose (33.8 ± 5.0 mg/L/OD_{600}).

Alcohol dehydrogenase selection

The second step in the *M. spicata* biosynthetic pathway is the NAD^+-dependent oxidation of (1*S*,5*R*)-carveol to (*R*)-carvone (Scheme 1), catalysed by (-)-isopiperitenol/(-)-carveol dehydrogenase (IPDH).[7] This alcohol dehydrogenase (ADH) is a member of the zinc-dependent short-chain dehydrogenase/ reductase superfamily similar to human 17β-hydroxysteroid dehydrogenase.[21] We performed *in vitro* biotransformations of cell lysates of IPDH expressed in *E. coli* strain BL21(DE3) with (1*S*,5*R*)- and (1*R*,5*R*)-carveol mix. Unfortunately only minor (*R*)-carvone yields were obtained, only ~2-fold higher than that obtained by constitutive *E. coli* ADHs alone (0.33 ± 0.17 *vs* 0.14 ± 0.01 μM). Therefore we cloned three additional IPDH homologues to identify the best performing enzyme capable of generating (*R*)-carvone in *E. coli*.

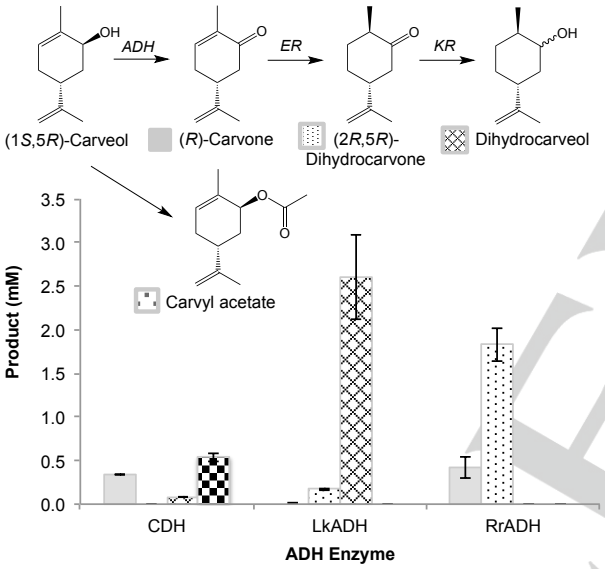

Figure 2. *In vitro* biotransformations of ADH enzymes in *E. coli* cell extracts, showing the proposed pathway of formation of by-products (2*R*,5*R*)-dihydrocarvone, dihydrocarveol isomers and carvyl acetate. The dihydrocarvone produced is ~ 90% (2*R*,5*R*)-isomer. No detectable native *E. coli* ADH activity with carveol was detected during *in vivo* reactions (Figure 1). *E. coli* enzymes ER and KR = ene-reductase and ketoreductase, respectively.

The first homologue was (1*S*,5*R*)-carveol dehydrogenase from *Rhodococcus erythropolis* DCL14 (CDH),[21] known to oxidise each of the 4 isomers of carveol, but with the highest affinity and turnover rate with the desired (1*S*,5*R*)-carveol. The second candidate was the ADH from *Rhodococcus ruber* DSM 44541 (RrADH), which is specific for a variety of (*S*)-secondary alcohols such as cyclohexanol.[22] The final homologue screened was the ADH from *Lactobacillus kefir* DSM 20587 (LkADH).[23] This enzyme differed by being $NADP^+$-dependent, (*R*)-selective, and required Mg^{2+} for activity. Prior studies with cell extracts of *E. coli* expressing LK-ADH showed a 21% conversion of a mixture of (1*S*,5*R*)- and (1*R*,5*R*)-carveol stereoisomers.[24]

Each gene was expressed in *E. coli* strain BL21(DE3), and clarified cell lysates were used for *in vitro* biotransformations with (1*S*,5*R*)- and (1*R*,5*R*)-carveol mix. Unfortunately, *E. coli* contains constitutive Old Yellow Enzymes and ketoreductases, which are likely to consecutively produce (2*R*,5*R*)-dihydrocarvone[25] and dihydrocarveol isomers, respectively from (*R*)-carvone (Figure 1A). Therefore evidence of each recombinant ADH activity above control cell lysates is apparent from the detection of one or more of three potential products.

Cell lysates of RrADH showed the highest yields of (*R*)-carvone (0.42 ± 0.13 mM), closely followed by CDH (0.34 ± 10 mM; Figure 1B). However, higher levels of by-products dihydrocarvone isomers (1.83 ± 0.19 mM) and neo-dihydrocarveol (2.6 ± 0.5 mM) were detected with enzymes RrADH and LkADH, suggesting high activity of the earlier ADH step. An additional by-product carvyl acetate (0.54 ± 0.05 mM) was seen in reactions with CDH lysate, presumably generated by the action of an *E. coli* alcohol acetyltransferase on carveol.[26] Therefore, potentially each of these ADH enzymes could be used to catalyse *in vivo* (1*S*,5*R*)-carveol dehydrogenation within *E. coli*.

(*S*)-Limonene to (*R*)-carvone operons

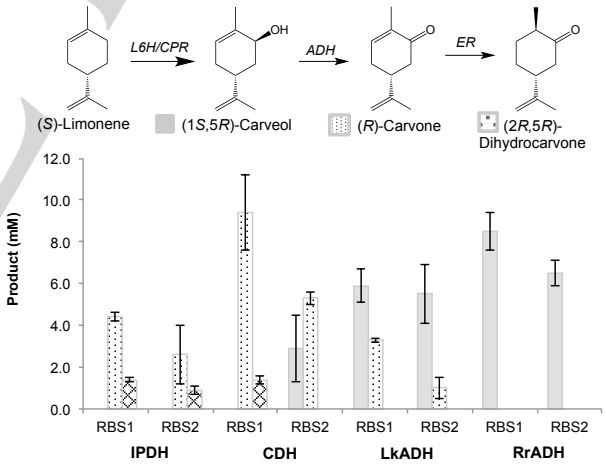

Figure 3. *In vivo* production of (*R*)-carvone and other monoterpenoids by $L6H_m$-SmCPR-ADH constructs in *E. coli*, co-expressed with limonene synthesis plasmid pJE16410, showing the proposed pathway of product formation. Cultures (5 mL) were grown in Terrific broth, containing phosphate salts (9.4 g/L KH_2PO_4 and 2.2 g/L K_2HPO_4), 0.7 % (w/v) glucose, 60 mg/mL kanamycin and 100 mg/mL ampicillin. The culture was incubated at 37°C, 200 rpm until reaching OD_{600} = 0.4, followed by 25 μM IPTG (pJE16410), 500 μM δ-aminolevulinic acid and 25 mM arabinose addition. Cultures were incubated at 30 °C for 72 hours. Culture aliquots (3 mL) were extracted with ethyl acetate (2 x 375 mL) containing 0.01 % *sec*-butyl benzene. Product yields and identification were determined by GCMS analysis.

The next stage involved combining the highest performing (1*S*,5*R*)-carveol-producing construct (L6H$_m$-SmCPR in pBbB8k) with the four ADH enzymes to find the optimal set of biocatalysts. Each operon was constructed by inserting the ADH gene downstream from SmCPR, separated by one of two ribosome binding sequences. RBS1 (GAATAACTATTTAAGAGGGAGAT TAATAACA) has a predicted translation rate of 13969,[27] while RBS2 (TAAGGAGGT) was chosen as it successfully increased the production of *p*-coumaryl alcohol in *E. coli* using a tricistronic operon.[28] Each construct was co-transformed with plasmid pJBEI6410 into *E. coli* strain NEB10β to screen for *in vivo* production of (*R*)-carvone from glucose.

Constructs containing CDH showed the highest levels of (*R*)-carvone production (71 ± 10 mg/L with RBS1). In contrast, IPDH-containing constructs showed a 2-fold reduction in yield (36.5 ± 1.8 with RBS1; Table 2). In both cases, (2*R*,5*R*)-dihydrocarvone was present due to the action of an *E. coli* ene-reductase. RrADH cultures only showed (1*S*,5*R*)-carveol presence, suggesting a lack of functional ADH protein expression. LkADH cultures also contained significant levels of (1*S*,5*R*)-carveol, with only moderate ADH activity detected (Table 2). Therefore, CDH was chosen as the biocatalyst for the *in vivo* production of (*R*)-carvone in *E. coli*.

Biocatalyst selection and screening for (2*R*,5*R*)-dihydrocarvone and (+)-DHCD production

The NADPH-dependent C=C reduction of (*R*)-carvone to (2*R*,5*R*)-dihydrocarvone is a well known reaction catalysed by OYE family members.[25, 29] We selected the classical OYE subclass member pentaerythritol tetranitrate reductase (PETNR) from *Enterobacter cloacae* PB2 as the biocatalyst for this step, as it is highly expressed in *E. coli* and is known to react with (*R*)-carvone to produce (2*R*,5*R*)-dihydrocarvone with high yields and diastereoselectivity (94% *de*).[30]

For the latter step, the flavin-dependent cyclohexanone monooxygenases (CHMO) catalyse the NADPH-dependent Baeyer−Villiger oxidation of cyclic ketones to form cyclic esters (lactones).[31] The CHMO from *Rhodococcus* species Phi1 (CHMO$_{WT}$) catalyses the oxidation of (2*R*,5*R*)-dihydrocarvone, however it generates the unwanted abnormal lactone (3*S*,6*S*)-6-isopropenyl-3-methyl-2-oxo-oxepanone.[32] Site directed mutagenesis studies of this enzyme generated a triple variant (F249A/F280A/F435A; CHMO$_{3M}$) that successfully produced the required 'normal' (+)-DHCD lactone.[8] Therefore we selected CHMO$_{3M}$ as the catalyst for the final lactone production step in *E. coli*.

To assess the performance of these two enzymes in *E. coli*, a variety of multi-gene constructs were generated and assessed for both (2*R*,5*R*)-dihydrocarvone and (+)-DHCD production under standard fermentation conditions. Cell extracts of each construct were tested by *in vitro* biotransformations in the presence of a commercially available (1*S*,5*S*)- and (1*R*,5*R*)-carveol mix, NAD$^+$ (IPDH) and an NADPH cofactor recycling system (PETNR and CHMO$_{3M}$). These early constructs contained the complete pathway from (*S*)-limonene to (+)-DHCD (L6H$_m$-IPDH-PETNR-CHMO$_{3M}$; L6H$_m$IPC$_{3M}$) except for CPR, as the most suitable CPR (and ADH homologue) had not been determined at the time of pathway construction. However the focus of these operon designs was to generate the most suitable PETNR-CHMO$_{3M}$ gene arrangement to maximise (+)-DHCD production from exogenously supplied (*R*)-carvone, so the absence of CPR and the presence of IPDH instead of CDH was inconsequential. Full details of the production of these constructs can be found in the Supporting Information Experimental sections 1-5 (Tables S1-S7 and Figures S1-S4).

Table 1. *In vitro* monoterpenoid production by L6HIPpC$_{3M}$ constructs with three different promoters upstream of CHMO$_{3M}$.[a]

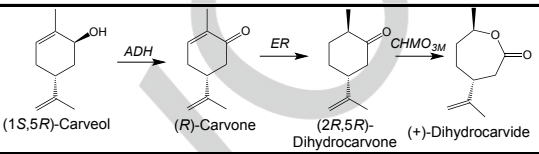

CHMO$_{3M}$ promoter	Substrate	(2*R*,5*R*)-DHC (mM)	(+)-DHCD (mM)	DHCL (mM)
trc/*lacO*[a]	Carveol	0.05 ± 0.01	0.12 ± 0.01	0.04 ± 0.01
	Carvone	2.36 ± 0.13	0.47 ± 0.06	trace
	DHC mix	-	0.57 ± 0.07	trace
PtetA	Carveol	0.11 ± 0.01	0.05 ± 0.02	0.03 ± 0.01
	Carvone	0.92 ± 0.15	0.28 ± 0.05	ND
	DHC mix	-	0.33 ± 0.06	ND
*rha*BAD	Carveol	0.15 ± 0.01	ND	0.41 ± 0.07
	Carvone	2.29 ± 0.07	0.11 ± 0.02	0.10 ± 0.02
	DHC mix	-	0.13 ± 0.03	ND

[a] No C-His$_6$-tag on PETNR. Reaction-s (1 mL) were performed in buffer (50 mM Tris pH 7.0) containing cell lysate, 5 mM (*R*)-carvone, 150 μM NAD$^+$ ± 15 μM NADP$^+$, 15 mM glucose and 10 U GDH. Reactions were incubated for 30 °C for 24 h at 130 rpm. Monoterpenoids were extracted with 2 x 0.5 mL ethyl acetate containing 0.1 % *sec*-butylbenzene internal standard. Product yields and identification were determined by GCMS analysis, using a DB-WAX column. No evidence was seen of native *E. coli* lactone formation. DHC mix = (2*R*,5*R*)- and (2*S*,5*R*)-dihydrocarvone; DHCD = dihydrocarvide lactone; DHCL = dihydrocarveol by-product. Trace = ≤ 0.02 mM. ND = none detected. The data for the production of (*R*)-carvone and by-product carvyl acetate is found in Supporting Information Tables S13-S14.

PETNR is known to be highly expressed and active in *E. coli* extracts,[33] so the main focus of the multiple L6H$_m$IPC$_{3M}$ designs was to increase the expression of CHMO$_{3M}$. An initial construct was generated with the genes under control of a single *lac*UV5 promoter (L6H$_m$IPC$_{3M}$). Biotransformations with carveol showed the production of (*R*)-carvone (0.87 ± 0.03 mM) and dihydrocarvone (0.34 ± 0.03 mM) above control *E. coli* extracts, the latter predominantly the (2*S*, 5*R*)-enantiomer (Supporting Information Table S11). No (+)-DHCD was detected, likely due to the low levels of the (2*S*, 5*R*)-dihydrocarvone substrate presence. To further check for CHMO$_{3M}$ expression, biotransformations were performed with (*R*)-carvone, eliminating the need for the IPDH step. This generated both (2*S*,5*R*)-dihydrocarvone (1.47 ± 0.08 mM) and (+)-DHCD (0.11 ± 0.01 mM), suggesting the presence of active CHMO$_{3M}$. However higher expression levels of CHMO$_{3M}$ are required to enable efficient (+)-DHCD production from earlier pathway intermediates. Three additional L6H$_m$IPC$_{3M}$ constructs were generated, where the ribosomal binding site sequence upstream

of $CHMO_{3M}$ was varied in an attempt to increase its expression levels. However no (+)-DHCD was detected during biotransformations, even in the presence of $CHMO_{3M}$ substrate (2*S*, 5*R*)-dihydrocarvone (Supporting Information Table S12).

The next approach to boost expression was to insert a variety of promoters upstream of $CHMO_{3M}$. The selected promoters were induced by IPTG (*trc*/*lacO*, *tacII*/*lacO*, *lac*UV5), rhamnose (*rha*BAD) or tetracycline (*PtetA*), allowing either a single (IPTG) control over expression of all 3 genes or differential control for $CHMO_{3M}$.[34] Biotransformations of cell extracts were performed with three different substrates to determine the most effective expression control system for $CHMO_{3M}$ (Table 1 and Supporting Information Tables S13-S14). As expected, in each case the highest (+)-DHCD production was seen in the presence of (2*S*, 5*R*)-dihydrocarvone ($CHMO_{3M}$ substrate), with the best yields obtained with $CHMO_{3M}$ under the control of a *trc*/*lacO* promoter (0.57 ± 0.07 mM; Table 1). When the $CHMO_{3M}$ promoter was substituted for *PtetA* and *rha*BAD, the yields decreased by 1.7- and 4.4-fold, respectively. Biotransformations in the presence of carveol showed a significant decrease in (+)-DHCD production (0.12 ± 0.01 mM with *trc*/*lacO*). In the case of the *rha*BAD-containing construct, no (+)-DHCD was produced in the presence of carveol. Therefore, the inclusion of the promoters *trc*/*lacO* and *PtetA* upstream of $CHMO_{3M}$ have successfully led to the production of (+)-DHCD from carveol.

Lactone production from glucose

Full pathway assembly was performed by using the most successful carvone-producing construct as the backbone ($L6H_m$-SmCPR-CDH RBS1; arabinose inducible), and inserting PETNR-promoter-$CHMO_{3M}$ genes downstream of CDH. Constructs L6HIP-*trc*-C_{3M} and L6HIP-*tet*-C_{3M} were chosen as the source of PETNR-promoter-$CHMO_{3M}$ genes due to their ability to produce (+)-DHCD in the presence of carveol. Additionally the L6HIP-*rha*-C_{3M} construct was chosen as it generated significant (+)-(+)-DHCD in the presence of (*R*)-carvone. The three dual promoter constructs (L6HCCP-*trc*-C_{3M}, L6HCCP-*tet*-C_{3M} and L6HCCP-*rha*-C_{3M}) were co-expressed in *E. coli* with the limonene synthesis plasmid for total *in vivo* production of (+)-DHCD lactone from glucose. Given the length of the number of steps in the pathway to (+)-DHCD, the addition of $CHMO_{3M}$ inducer was added either at the same time as the other inducers (IPTG and arabinose), or 6 h later, to give time for the intermediate monoterpenoid concentrations to build up within the cell. As the *trc*-promoter is IPTG inducible, the expression of $CHMO_{3M}$ in construct L6HCCP-*trc*-C_{3M} could not be postponed for 6 hours as IPTG is required for the induction of the limonene synthesis genes (pJBEI6410 plasmid).

In vivo studies showed two of the three construct combinations successfully generated (+)-DHCD from glucose (Figure 4). The most successful limonene to lactone-producing construct in *E. coli* was L6HCCP-*rha*-C_{3M}, which showed around 6 mg/L (+)-DHCD, dependent on the induction conditions. Interesting, the highest *in vitro* (+)-DHCD-producing construct L6HCCP-*trc*-C_{3M} did not show any detectable levels of (+)-DHCD under *in vivo* conditions when co-expressed with the limonene-producing plasmid. This highlights the importance of screening multiple constructs with different controlling elements, as the addition of an extra IPTG-inducible pathway can sometimes (unpredictably) impact on the expression of each recombinant gene.

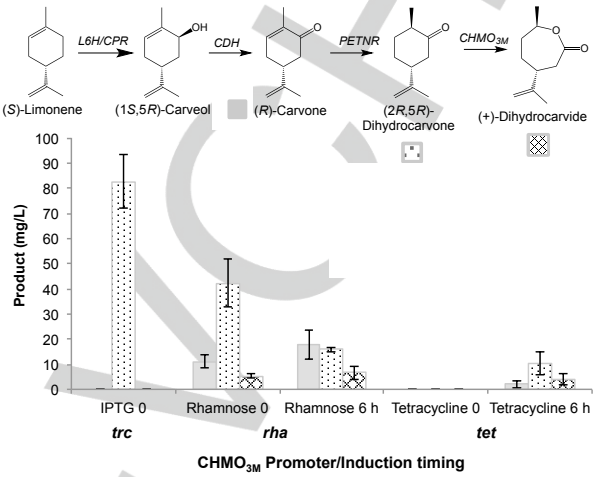

Figure 4. *In vivo* monoterpenoid production from limonene by $L6CCPpC_{3M}$ constructs with three different promoters upstream of $CHMO_{3M}$, co-expressed with limonene synthesis plasmid pJE16410. Cultures (5 mL) were grown in Terrific broth, containing phosphate salts (9.4 g/L KH_2PO_4 and 2.2 g/L K_2HPO_4), 0.7 % (w/v) glucose, 60 μg/mL kanamycin and 100 μg/mL ampicillin. The culture was incubated at 37°C, 200 rpm until reaching OD600 = 0.4, followed by the addition of 25 μM IPTG (pJE16410), 500 μM δ-aminolevulinic acid, 25 μM arabinose and either 0.05% rhamnose or 100 nM tetracycline at the time of induction of after 6 hours. Cultures were incubated at 30 °C for 72 hours. Aliquots (3 mL) were extracted with ethyl acetate (2 x 375 μL) containing 0.01 % *sec*-butyl benzene. Product yields and identification were determined by GCMS analysis.

Conclusions

In vivo production of fine chemicals is one possible solution to the increasing demand for sustainable and renewable manufacturing. The cost-effectiveness of biological manufacturing strategies is dependent on the construction of recombinant microorganisms expressing the correct 'assembly line' of enzymes at sufficient levels. We have achieved a proof of principle demonstration of *in vivo* production of bioplastics precursor (+)-DHCD in *E. coli*, grown on a simple, inexpensive carbon source. This overcomes the severe limitations in the existing partial pathway approach (limonene to lactone) caused by the addition of a cytotoxic precursor (limonene) supply to the microorganism.[13] The *in vivo* production of limonene in *E. coli* overcomes the precursor uptake constraints, and minimises cytotoxicity by the effective removal of the precursor molecules by the remaining pathway steps.

Further studies are required to increase the productivity and cost-effectiveness of this bio-manufacturing approach to bioplastics production. This is necessary to increase the production titres, concomitant with the elimination of selection agents (antibiotics) and expensive chemical induction (e.g. IPTG and rhamnose). For example, host selection and (chromosomal)

modification could be applied to reduce the cytotoxicity and recovery of the monoterpenoids and by increasing cellular export. A high throughput combinatorial approach could be applied to screen for the best combination of enzyme homologues/variants, vector backbone, promoter combination and gene order. However our demonstration of the complete *in vivo* production of (+)-DHCD is a leap forward in the development of truly sustainable and renewable bioplastic monomers.

Experimental Section

General materials and reagents: All chemicals and solvents were purchased from commercial suppliers, and were of analytical grade or better. Media components were obtained from Formedium (Norfolk, UK). Gene sequencing and oligonucleotide syntheses were both performed by Eurofins MWG (Ebersberg, Germany). The BglBrick series of vectors and the mevalonate pathway overexpression plasmid pJBEI6410[15a] were obtained from Addgene (https://www.addgene.org).[34]

Gene synthesis and sub cloning: The genes encoding the C-terminally His_6-tagged proteins pentaerythritol tetranitrate reductase (PETNR C-His_6) from *Enterobacter cloacae* (UNIPROT: P71278)[35] and cyclohexanone monooxygenase ($CHMO_{WT}$) from *Rhodococcus* species Phi1 (UNIPROT: Q84H73)[8] were synthesised and sub cloned into pET21b as described previously. The CHMO triple variant F249A/F280A/F414A ($CHMO_{3M}$) was generated by PCR mutagenesis as described previously.[8] The following C-terminally His_6-tagged alcohol dehydrogenase genes were synthesised and sub cloned into pET21b by GenScript: (-)-*trans*-isopiperitenol dehydrogenase from *Mentha piperita* (IPDH; UNIPROT: Q5C919),[7] (1*S*,5*R*)-carveol dehydrogenase from *Rhodococcus erythropolis* (CDH; UNIPROT: Q9RA05),[21] (*R*)-specific alcohol dehydrogenase from *Lactobacillus kefir* (LkADH; UNIPROT: Q6WVP7)[36] and secondary alcohol dehydrogenase from *Rhodococcus ruber* DSM 44541 (Rr-ADH; UNIPROT: Q8KLT9).[23] Each gene was codon optimised for optimal expression in *E. coli*. In the case of IPDH, a stop codon was inserted before the *Xho*I site by overlap extension PCR[37] to eliminate the C-terminal His_6-tag.

The gene encoding an N-terminally modified mature (4*S*)-limonene-6-hydroxylase from *M. spicata* ($L6H_m$; UNIPROT: Q9XHE8)[17] was synthesised and sub cloned without codon optimisation into pCWori (+) by Geneart. The N-terminus was modified by the removal of the chloroplast signal sequence in addition to other modifications designed to increase the soluble expression in *E. coli* as described previously.[17] Two C-terminally His_6-tagged cytochrome P450 reductases from *Arabidopsis thaliana* (AtCPR; UNIPROT: Q9SB48) and *Salvia miltiorrhiza* (SmCPR), (UNIPROT:S4URU2) were synthesised and sub cloned into pET21b, incorporating codon optimisation techniques of rare codon removal. Each gene was transformed into competent cells of *E. coli* strain BL21(DE3) for functional overexpression according to the manufacturers protocols.

Limonene hydroxylation construct assembly: Functional limonene hydroxylation constructs were generated by In-Fusion cloning (Takara)[38] between PCR linearised $L6H_m$ (3' end) in pCWori (+) and either AtCPR or SmCPR, with the inclusion of a Shine-Dalgarno sequence between the genes ($L6H_m$-AtCPR and $L6H_m$-SmCPR, respectively). The constructs were transformed into *E. coli* strain JM109 for functional expression. The two constructs were further sub cloned into vectors pBbB8k-RFP and pBbE2k-RFP (Addgene)[34] under the control of a tetracycline and pBAD promoters, respectively. This was performed using In-Fusion cloning between PCR linearised vector (RFP eliminated) and an L6H-CPR insert. Following each PCR reaction, template removal was performed by DpnI digestion, and PCR product size was determined by 0.6% agarose gel electrophoresis. The oligonucleotide sequences encoding all the PCR primers can be found in Supporting Information Table S1. The correct assembly of each construct was confirmed by DNA sequencing. Each construct was co-transformed with plasmid pJBEI6410 into competent cells of *E. coli* strain NEB10β for functional overexpression according to the manufacturers protocols.

Production and *in vitro* biotransformations of ADH lysates: ADH clones were grown in LB (10 g/L tryptone, 5 g/L yeast extract and 5 g/L NaCl) containing 100 μg/mL ampicillin and starter culture (2%). In the case of CDH production, 182 g/L sorbitol and 0.293 g/L betaine-HCl were included in the medium. Cultures were incubated at 37°C until OD600 nm = 0.5. Protein production was induced by the addition of 100 μM IPTG, followed by incubation at 30 °C for 16-18h. Cells were harvested by centrifugation (4000 x *g*) and the pellets were resuspended in 1.7 mL lysis buffer (50 mM Tris pH 7.0 containing the EDTA-free complete protease inhibitor cocktail, 1 mM $MgCl_2$, 0.1 mg/mL DNase I, 0.1 mg/mL lysozyme and 10% glycerol). Cell-free supernatants were generated by sonication (10 cycles of 10 s on/1 min off at 40 % amplitude) and centrifugation for 5 minutes (13,000 *g*). The presence of the individual recombinant proteins was determined by SDS PAGE, using 12% Mini-PROTEAN-TGX stain-free gels (Bio-Rad). Protein content was visualised using a Safe Imager 2.0 Blue light trans illuminator (Bio-Rad).

Reactions (1 mL) were performed in buffer (50 mM Tris pH 7.0) containing 5 mM (1*S*,5*R*)- and (1*R*,5*R*)-carveol mix, 15 μM $NADP^+$, 15 mM glucose and 10 U GDH. Reactions were incubated at 30 °C for 72 h at 130 rpm. Control reactions were performed with *E. coli* lysates that did not contain the recombinant plasmids. In each case, monoterpenoids were extracted with 2 x 0.5 mL ethyl acetate containing 0.1 % *sec*-butylbenzene internal standard. Product yields and identification were determined by GC and GCMS analysis, respectively, using a DB-WAX column.

Generation of the L6H-CPR-ADH constructs: Eight constructs were generated whereby each ADH was inserted downstream of the CPR gene of $L6H_m$-SmCPR in pBbB8k preceded by one of two different ribosome binding sequences (rbs 1-2). This was performed using In-Fusion cloning between PCR linearised $L6H_m$-SmCPR and amplified rbs-ADH insert ($L6H_m$-SmCPR-IPDH, $L6H_m$-SmCPR-CDH, $L6H_m$-SmCPR-LkADH and $L6H_m$-SmCPR-RRADH versions 1 and 2, respectively). Following each PCR reaction, template removal and DNA clean up was performed as above. The oligonucleotide sequences encoding the PCR primers can be found in Supporting Information Table S2. The correct assembly of each construct was confirmed by DNA sequencing. Each construct was co-transformed with plasmid pJBEI6410 into competent cells of *E. coli* strain NEB10β for functional overexpression according to the manufacturers protocols.

Construction of multi-enzyme cascade constructs containing PETNR and $CHMO_{3M}$: A series of multi-gene constructs containing $L6H_m$, IPDH, PETNR and $CHMO_{WT}$ or $CHMO_{3M}$ were generated to maximise the production of (+)-DHCD lactone from (1*S*,5*R*)-carveol. Optimisation parameters varied were the plasmid backbone (pBbE1c or pBbE5c), RBS sequences and the presence of 4 different promoters upstream of $CHMO_{3M}$. Full details of the assembly techniques and biotransformation data performed for each construct can be found in the Supporting Information document.

Construction of the complete lactone producing pathway from limonene: (+)-DHCD producing constructs from (*S*)-limonene (Supporting Information Figure S5) were generated by In-Fusion cloning between the PCR linearised $L6H_M$-SmCPR-CDH construct (contains rbs 1) in pBbB8k and one of three PETNR-promoter-$CHMO_{3M}$ inserts amplified from L6HIP-*tet*-C_{3M}, L6HIP-*rha*-C_{3M} and L6HIP-*trc*-C_{3M}. These inserts differ by the type of promoter located upstream of the $CHMO_{3M}$

gene, which are tetracycline-, rhamnose- and IPTG-inducible, respectively. PCR linearisation of L6H$_M$-SmCPR-CDH was performed between the 3' end of CDH and the terminator region, while amplification of the PETNR-*promoter*-CHMO$_{3M}$ inserts included rbs2 upstream of PETNR. Following each PCR reaction, template removal and DNA clean up was performed as above. The oligonucleotide sequences encoding the PCR primers can be found in Supporting Information Table S8. The correct assembly of each construct was confirmed by DNA sequencing (L6HCCP-*tet*-C$_{3M}$, L6HCCP-*rha*-C$_{3M}$ and L6HCCP-*trc*-C$_{3M}$). Each construct was co-transformed with plasmid pJBEI6410 into competent cells of *E. coli* strain NEB10β for functional overexpression according to the manufacturers protocols. A summary of all the gene constructs is found in Supporting Information Table S9.

***In vivo* biotransformations:** A single colony of *E. coli* NEB10β co-transformed with pJBEI6410 and pBbB8k-containing biosynthetic constructs was used to inoculate 5 mL of Terrific broth, containing phosphate salts (9.4 g/L KH_2PO_4 and 2.2 g/L K_2HPO_4), 0.7 % (w/v) glucose 60 μg/mL kanamycin and 100 μg/mL ampicillin. The culture was incubated at 37°C, and 200 rpm until reaching OD600 = 0.4, followed by IPTG, arabinose, δ-aminolevulinic acid ± tetracycline addition ± rhamnose (25 μM, 25 mM, 500 μM, 100 nM and 0.05%, respectively). The cultures were incubated at 30 °C for 72 hours unless otherwise stated. Each culture aliquot (3 mL) was cooled for 10 minutes on ice, followed by extraction with ethyl acetate (2 x 375 μL) containing 0.0[8]1 % *sec*-butyl benzene. Product yields and identification were determined by GCMS analysis.

Analytical techniques: Monoterpenoid content quantification was performed using an Agilent Technologies 7890A GC system with an FID detector. Biotransformation extracts (1 mL) were analysed on a DB-WAX column (30 m; 0.32 mm; 0.25 μm film thickness; JW Scientific). In this method the injector temperature was at 220 °C with a split ratio of 20:1. The carrier gas was helium with a flow rate of 1 mL/min and a pressure of 5.1 psi. The program began at 40°C with a hold for 2 minutes, followed by an increase of temperature to 210°C at a rate of 15°C/minute, with a final hold at 210 °C for 3 min. The FID detector was maintained at a temperature of 250°C with a flow of hydrogen at 30 mL/min. Product quantitation was performed by comparing the peak areas to those of authenticated standards of known concentration. Where authentic standards were not commercially available (by-products only), the concentrations were estimated using an average concentration per peak area value based on 11 related monoterpenoid standards.

Monoterpenoid identification was performed on an Agilent Technologies 7890B GC system with a 5977A MSD extractor EI source detector using the same DB-WAX column. In this method the injector temperature was at 240°C with a split ratio of 50:1. The carrier gas was helium with a flow rate of 3 mL/min and a pressure of 8.3 psi. The program began at 50 °C with a hold for 1 min followed by an increase of temperature to 68 °C at a rate of 5 °C/minute, with a hold at 68 °C for 2 min. A second temperature gradient was applied at 25 °C/minute until 230 °C with a final hold of 2 minutes. The mass spectra fragmentation patterns were entered into the NIST/EPA/NIH 11 mass spectral library for identification of a potential match.

Upscaled *in vitro* biotransformations and analysis: Reactions (10 mL) were performed in buffer (50 mM Tris pH 7.0) containing (*R*)-carvone/(+)-dihydrocarvone starting substrate (5 mM; ~30 mg), $NADP^+$ (10 mM), glucose (15 mM), GDH (10 U) and the enzyme(s) (10 μM). The samples were incubated at 30 °C for 24 h at 180 rpm, cooled in ice, and the organic compound(s) were extracted with petroleum ether (PET; 1:2 (v/v) ratio). Two further PET extractions were performed, and the pooled organic phase was dried with anhydrous $MgSO_4$. The product(s) were recovered following solvent removal using a rotor evaporator with the water bath set to 30 °C, at 20-30 torr. Product(s) purification was performed chromatographically on silica gel (pore size 60, 220-240 mesh size, particle size 35-75 μm), which was equilibrated with 100% PET. The compounds were eluted with a mix of PET and ether (5-40%), and each elution fraction was analysed by thin-layer chromatography (TLC) using a mobile phase composed of a PET/ether in 70:30 ratio. The TLC plate was stained with phosphomolybdic acid stain (PMA; 12 g in 250 mL ethanol) and exposed to UV-light. The fractions containing the desirable metabolites were pooled, and the solvent was removed as before.

^{1}H and ^{13}C NMR spectra of the up-scaled purified product(s) (10 mg/mL) in deuterated chloroform were recorded on a Bruker Avance 400 MHz NMR spectrometer at 298 K without the addition of an internal standard. Chemical shifts are reported as δ in parts per million (ppm) and are calibrated against the residual solvent signal. ^{1}H AND ^{13}NMR spectra were analysed using MestreNova.

Acknowledgements

This work was funded by grants provided by the BBSRC and EPSRC (BB/M000354/1 and BB/M017702/1). UK Catalysis Hub is kindly thanked for resources and support provided via our membership of the UK Catalysis Hub Consortium and funded by EPSRC (grants EP/K014706/2, EP/K014668/1, EP/K014854/1, EP/K014714/1 and EP/M013219/1)'

Keywords: (+)-Dihydrocarvide monomer • Baeyer-Villiger monooxygenases • synthetic biology • bioplastics • engineering

[1] a) A. Gandini, T. M. Lacerda, *Prog. Polym. Sci.* **2015**, *48*, 1-39; b) S. A. Miller, *ACS Macro Lett.* **2013**, *2*, 550-554.
[2] Y. Zhu, C. Romain, C. K. Williams, *Nature* **2016**, *540*, 354-362.
[3] M. Labet, W. Thielemans, *Chem. Soc. Rev.* **2009**, *38*, 3484-3504.
[4] A. P. Gupta, V. Kumar, *Eur. Polym. J.* **2007**, *43*, 4053-4074.
[5] a) K. J. Zhu, X. Z. Lin, S. L. Yang, *J. Appl. Polym. Sci.* **1990**, *39*, 1-9; b) M. Vert, S. M. Li, G. Spenlehauer, P. DGuerin, *J. Mater. Sci.: Mater. Med.* **1992**, *3*, 432-446; c) P. Mainil-Varlet, B. Rahn, S. Gogolewski, *Biomaterials* **1997**, *18*, 257-266.
[6] S. A. Gurusamy-Thangavelu, S. J. Emond, A. Kulshrestha, M. A. Hillmyer, C. W. Macosko, W. B. Tolman, T. R. Hoye, *Polym. Chem.* **2012**, *3*, 2941-2948.
[7] K. L. Ringer, E. M. Davis, R. Croteau, *Plant Physiol.* **2005**, *137*, 863-872.
[8] H. L. Messiha, S. T. Ahmed, V. Karuppiah, R. Suardiaz, G. A. Avalos, N. Fey, S. Yeates, H. S. Toogood, A. J. Mulholland, N. S. Scrutton, *Biochemistry* **2018**, *57*, 1997-2008.
[9] J. R. Lowe, W. B. Tolman, M. A. Hillmyer, *Biomacromolecules* **2009**, *10*, 2003-2008.
[10] a) M. J. L. Tschan, E. Brule, P. Haquette, C. M. Thomas, *Polym. Chem.* **2012**, *3*, 836-851; b) M. A. Hillmyer, W. B. Tolman, *Acc. Chem. Res.* **2014**, *47*, 2390-2396.
[11] D. Zhang, M. A. Hillmyer, W. B. Tolman, *Biomacromolecules* **2005**, *6*, 2091-2095.
[12] a) K. Balke, M. Baeumgen, U. T. Bornscheuer, *ChemBioChem* **2017**, *18*, 1627-1638; b) K. Balke, M. Kadow, H. Mallin, S. Saß, U. T. Bornscheuer, *Org. Biomol. Chem.* **2012**, *10*, 6249-6265; c) H. Leisch, K. Morley, P. C. K. Lau, *Chem. Rev. (Washington, DC, U. S.)* **2011**, *111*, 4165-4222; d) N. Oberleitner, A. K. Ressmann, K. Bica, K. Gartner, P. Gartner, M. W. Fraaije, U. T. Bornscheuer, F. Rudroff, M. D. Mihovilovic, *Green Chem.* **2017**, *19*, 367-371.
[13] O. A. Carter, R. J. Peters, R. Croteau, *Phytochemistry* **2003**, *64*, 425-433.

[14] A. Casini, F.-Y. Chang, R. Eluere, A. King, E. M. Young, Q. M. Dudley, A. Karim, K. Pratt, C. Bristol, A. Forget, A. Ghodasara, R. Warden-Rothman, R. Gan, A. Cristofaro, A. E. Borujeni, M.-H. Ryu, A.-T. J. Li, Y. C. Kwon, H. Wang, E. Tatsis, C. Rodriguez-Lopez, S. O'Connor, M. H. Medema, M. Fischbach, M. C. Jewett, C. A. Voigt, B. Gordon, *J. Am. Chem. Soc.* **2018**, *140*, 4302–4316.

[15] a) J. Alonso-Gutierrez, R. Chan, T. S. Batth, P. D. Adams, J. D. Keasling, C. J. Petzold, T. S. Lee, *Metab. Eng.* **2013**, *19*, 33-41; b) T. P. Korman, P. H. Opgenorth, J. U. Bowie, *Nat. Commun.* **2017**, *8*, 1-8.

[16] S. Lupien, F. Karp, M. Wildung, R. Croteau, *Arch. Biochem. Biophys.* **1999**, *368*, 181-192.

[17] C. Haudenschild, M. Schalk, F. Karp, R. Croteau, *Arch. Biochem. Biophys.* **2000**, *379*, 127-136.

[18] B. M. Lange, M. R. Wildung, E. J. Stauber, C. Sanchez, D. Pouchnik, R. Croteau, *Proc. Natl. Acad. Sci. U. S. A.* **2000**, *97*, 2934-2939.

[19] J. Glazyrina, E. M. Materne, T. Dreher, D. Storm, S. Junne, T. Adams, G. Greller, P. Neubauer, *Microb. Cell Fact.* **2010**, *9*, 42.

[20] N. G. H. Leferink, A. J. Jervis, Z. Zebec, H. S. Toogood, S. Hay, E. Takano, N. S. Scrutton, *ChemistrySelect* **2016**, *1*, 1893-1896.

[21] M. J. van der Werf, C. van der Ven, F. Barbirato, M. H. Eppink, J. A. de Bont, W. J. van Berkel, *J. Biol. Chem.* **1999**, *274*, 26296-26304.

[22] C. Hamnevik, C. Blikstad, S. Norrehed, M. Widersten, *J. Mol. Catal. B: Enzym.* **2014**, *99*, 68-78.

[23] W. Hummel, A. Riebel, *Ann. N. Y. Acad. Sci.* **1996**, *799*, 713-716.

[24] N. Oberleitner, C. Peters, J. Muschiol, M. Kadow, S. Saß, T. Bayer, P. Schaaf, N. Iqbal, F. Rudroff, M. D. Mihovilovic, U. T. Bornscheuer, *ChemCatChem* **2013**, *5*, 3524-3528.

[25] H. S. Toogood, J. M. Gardiner, N. S. Scrutton, *ChemCatChem* **2010**, *2*, 892-914.

[26] A. Aharoni, L. C. P. Keizer, H. J. Bouwmeester, Z. Sun, M. Alvarez-Huerta, H. A. Verhoeven, J. Blaas, A. M. M. L. van Houwelingen, R. C. H. De Vos, H. van der Voet, R. C. Jansen, M. Guis, J. Mol, R. W. David, M. Schena, A. J. van Tunen, A. P. O'Connell, *Plant Cell* **2000**, *12*, 647-661.

[27] H. M. Salis, E. A. Mirsky, C. A. Voigt, *Nat. Biotechnol.* **2009**, *27*, 946–950.

[28] P. V. van Summeren-Wesenhagen, R. Voges, A. Dennig, S. Sokolowsky, S. Noack, U. Schwaneberg, J. Marienhagen, *Microb. Cell Fact.* **2015**, *14*, 79-88.

[29] H. S. Toogood, D. Mansell, J. M. Gardiner, N. S. Scrutton, in *Comprehensive Chirality*, 1 ed. (Eds.: H. Yamamoto, E. Carreira), Elsevier Science, Oxford, **2011**, pp. 216-260.

[30] H. S. Toogood, A. Fryszkowska, M. Hulley, M. Sakuma, D. Mansell, G. M. Stephens, J. M. Gardiner, N. S. Scrutton, *ChemBioChem* **2011**, *12*, 738-749.

[31] D. Sheng, D. P. Ballou, V. Massey, *Biochemistry* **2001**, *40*, 11156-11167.

[32] P. C. Brzostowicz, D. M. Walters, S. M. Thomas, V. Nagarajan, P. E. Rouvière, *Appl. Environ. Microbiol.* **2003**, *69*, 334-342.

[33] H. S. Toogood, A. Ní Cheallaigh, S. Tait, D. J. Mansell, A. Jervis, A. Lygidakis, L. Humphreys, E. Takano, J. M. Gardiner, N. S. Scrutton, *ACS Synth. Biol.* **2015**, *4*, 1112-1123.

[34] T. S. Lee, R. A. Krupta, F. Zhang, M. Hajimorad, W. J. Holtz, N. Prasad, S. K. Lee, J. D. Keasling, *J. Biol. Eng.* **2011**, *5*, 12.

[35] M. E. Hulley, H. S. Toogood, A. Fryszkowska, D. Mansell, G. M. Stephens, J. M. Gardiner, N. S. Scrutton, *ChemBioChem* **2010**, *11*, 2433-2447.

[36] W. Stampfer, B. Kosjek, C. Moitzi, W. Kroutil, K. Faber, *Angew. Chem., Int. Ed. Engl.* **2002**, *41*, 1014–1017.

[37] Y.-H. Xiao, M.-H. Yin, L. Hou, M. Luo, Y. Pei, *Biotechnol. Lett.* **2007**, *29*, 925-930.

[38] A. L. Throop, J. LaBaer, *Curr. Protoc. Mol. Biol.* **2015**, *110*, 3.20.21-23.20.23.

Entry for the Table of Contents (Please choose one layout)

Layout 1:

FULL PAPER

Text for Table of Contents

*Gabriel A. Ascue Avalos, Helen S. Toogood, Shirley Tait, Hanan L. Messiha and Nigel S. Scrutton **

From bugs to bioplastics: Total (+)-dihydrocarvide biosynthesis by engineered *Escherichia coli*